GEOPHYSICAL RESEARCH LETTERS, VOL. 33, L21313, doi:10.1029/2006GL027850, 2006

Fault slip rates from three-dimensional models of the Los Angeles metropolitan area, California

Michele L. Cooke[1] and Scott T. Marshall[1]

Received 16 August 2006; accepted 5 October 2006; published 9 November 2006.

[1] We present results from the first mechanical model of active tectonics in the Los Angeles region to use non-planar, geologically representative fault surfaces compiled by the Southern California Earthquake Center Community Fault Model. The fault slip rates from our three-dimensional model match well the available geologic slip rates. Discrepancies in reverse slip along the Upper Elysian Park fault and strike-slip along the Raymond fault may reflect imprecise knowledge of local fault geometry. Discrepancy in the average dip slip rate along the Palos Verdes fault reveals variations in dip slip along that surface; model predictions at the location of the geological investigation have good match to geologic data. The validated model is used to estimate dip and strike slip rates for 26 active faults in the Los Angeles metropolitan region, many of which are otherwise unconstrained by geologic evidence. **Citation:** Cooke, M. L., and S. T. Marshall (2006), Fault slip rates from three-dimensional models of the Los Angeles metropolitan area, California, *Geophys. Res. Lett.*, *33*, L21313, doi:10.1029/2006GL027850.

1. Introduction

[2] Seismic hazard assessments used to estimate earthquake risk require characterization of the seismic source, specifically the earthquake magnitude and recurrence rates of potentially damaging earthquakes [*Working Group on California Earthquake Probabilities*, 1995]. The probable magnitude and recurrence rate are, in turn, typically inferred from more direct measurements such as slip rates along faults [e.g., *Grant and Gould*, 2004]. While slip rates have been either measured from rupture evidence at specific sites or inferred from associated deformation along more than 13 active faults within the Los Angeles metropolitan region (Tables 1 and 2), significant knowledge gaps remain (Auxiliary material).[1] For example, strike-slip rates along blind faults, such as the Puente Hills Thrust fault, are nearly impossible to determine from the information available. Three-dimensional numerical models that simulate the geologic deformation may fill this knowledge gap and provide the suitable estimates for slip rates along under-characterized faults.

[3] The Los Angeles metropolitan region hosts multiple systems of active faults that cannot be accurately simulated by two-dimensional models. Northwest-southeast trending strike-slip and reverse faults of the Peninsular ranges abut east-west trending reverse faults of the transverse ranges [e.g., *Wright*, 1991] resulting in a network of oblique and intersecting active faults with complex three-dimensional surfaces [e.g., *Plesch et al.*, 2002]. Detailed surfaces for active faults in Southern California have been compiled within the Southern California Earthquake Center's (SCEC) Community Fault Model (CFM) [*Plesch et al.*, 2002]. Faults of this dataset are defined at the highest resolution available from geologic maps, wells and seismic reflection data. The CFM reveals the imbricate nature of thrust faults as well as the complex intersection of obliquely trending faults (Figure 1). Two dimensional interseismic models of the Los Angeles basin, with a single planar fault have matched aspects of the geodetic signal [*Argus et al.*, 2005]; however the simple fault geometry within that model produces unreasonably high geologic slip rates (8 mm/yr [*Argus et al.*, 2005] much greater than 1.7 mm/yr [*Shaw et al.*, 2002]). By incorporating the complexity of the Los Angeles basin fault system within a mechanical model of geologic deformation we are able to simulate the distribution of geologic deformation and estimate complete slip rates (dip, strike and net) on all of the regional faults.

[4] In this paper, we develop a three-dimensional Boundary Element Method (BEM) model of the non-planar and oblique fault system of the Los Angeles region that preserves complex geologically-constrained fault topology. This is the first model of three-dimensional deformation along all of the non-planar active fault systems within Los Angeles. We are able to achieve this milestone by using BEM, which only requires meshing of fault surfaces and is less labor intensive than creating a comparable FEM model, which requires a volumetric mesh. We validate the model by comparing the predicted fault slip rates to available geologic slip rates. The validated BEM model results can be used to estimate representative slip rates on faults along which slip is otherwise geologically unconstrained.

2. Three-Dimensional Models

[5] To preserve the non-planar and complex topology of the tessellated CFM fault surfaces, we use a triangular element formulation of the Boundary Element Method implemented in POLY3D [*Thomas*, 1994]. This method embeds irregular fault surfaces within a linear-elastic half-space. Deformation can result from either remote stress/strain or driving slip/stresses along the fault surfaces. POLY3D has been used to simulate the three-dimensional active tectonics of the Marmara Sea [*Muller and Aydin*, 2005], the Hector Mine earthquake [*Maerten et al.*, 2005]

[1]Geosciences Department, University of Massachusetts, Amherst, Massachusetts, USA.

0094-8276/06/2006GL027850$05.00

[1]Auxiliary material data sets are available at ftp://ftp.agu.org/apend/gl/2006gl027850. Other auxiliary material files are in the HTML.

Table 1. Geologic Reverse-Slip Rates[a]

Fault Name	Low Rate Limit, mm/yr	High Rate Limit, mm/yr
Puente Hills Thrust	0.4	1.7
Santa Monica	0.5	1.3
Northridge	1.0	2.0
Cucamonga	4.5	*uncertain*
Sierra Madre		
East	0.6	5.0
West	0.6	2.2
Upper Elysian Park	0.58	2.2
Palos Verdes	0.26	0.35; 0.38

[a]See C. J. Wills et al., Fault Section Database 2.0., Working Group of California Earthquake Probabilities, 2006, http://gravity.usc.edu/WGCEP/modelComponents/deformModels/index.html, and references therein. Primary references are listed in auxiliary material Text S1.

and the Los Angeles basin [*Griffith and Cooke*, 2004, 2005].

[6] We remesh the CFM surfaces to provide more uniform element size and to ensure coincident nodes at fault intersections. The average diameter of elements within our model is 3 km, sufficient to represent >10 km scale geometric complexities that influence slip distribution.

[7] The geologic evidence used to determine fault slip rates, such as offset layers within trenches and geomorphic expressions of faulting, reflect the sum effect of coseismic slip of faults within the seismogenic crust and any aseismic fault slip or viscous flow of material below the brittle-ductile transition. For this reason, we extend the fault surfaces, which in the CFM are only defined to 18 km depth, to a horizontal freely-slipping detachment at 27.5 km. This detachment sits near the inferred depths of the Moho in the region [*Fuis et al.*, 2001; *Magistrale et al.*, 2000] and serves to decouple the overlying deformation so that fault slip is not resisted by the half-space formulation of the BEM models. The edges of the detachment are positioned sufficiently far away as to have no influence on deformation within the Los Angeles basin. Within this mechanical model, the entire fault surfaces are free to slip and interact under the remotely applied tectonic loading.

[8] Remote strain is applied to the model in order to simulate the regional tectonic deformation determined from GPS stations at the edges of the Los Angeles region. After the effects of the San Andreas fault, San Jacinto fault and fluid pumping are removed, stations at the Palos Verdes peninsula are moving 6–7 mm/year northward relative to the San Gabriel mountain stations ~70 km away [*Argus et al.*, 2005]. To the models we apply remote contraction of 90 nanostrain/year at N9°E orientation, which reflects the average azimuth of station movement relative to the San Gabriel Mountains [*Argus et al.*, 2005]. These conditions simulate vertical thickening of the region, which produces good overall match to slip sense of faults in the Los Angeles basin and better match than conditions of east-west extension [*Griffith and Cooke*, 2005]. This and previous studies [*Griffith and Cooke*, 2004, 2005] simulate geologic deformation using tectonic boundary conditions that are determined from geodesy over the past ~10 years. If the past 10 years of deformation is not representative of geologic strain accumulation, the model boundary conditions would require revision.

[9] Unlike kinematic analyses, which require that the sum of fault slip rates equals the measured geodetic deformation [*Meade and Hager*, 2005], mechanical models explicitly include off-fault deformation so that fault slip rates may not sum to the geodetic rates. The remaining off-fault deformation can be accommodated within the host rock between faults as folding, fracturing and pervasive fabric development. Mechanical models, unlike kinematic models, are equipped to incorporate off-fault strain partitioning.

Table 2. Geologic Strike-Slip Rates[a]

Fault Name	Slip Sense	Low Rate Limit, mm/yr	High Rate Limit, mm/yr
Palos Verdes	right-lateral	2.5; 2.7	3.0; 3.8
Newport-Inglewood	right-lateral	0.3	1.5
Hollywood	left-lateral	0.35	*uncertain*
Raymond	left-lateral	1.5	*uncertain*
Whittier	right-lateral	1.0	3.0
Chino	right-lateral	0.35	1.9
San Gabriel	right-lateral	1.0	2.5

[a]See C. J. Wills et al., Fault Section Database 2.0., Working Group of California Earthquake Probabilities, 2006, http://gravity.usc.edu/WGCEP/modelComponents/deformModels/index.html, and references therein. Primary references are listed in auxiliary material Text S1.

3. Model Validation by Correlation of Fault Slip Rates

[10] To validate the models, we compare the average fault slip rates along the entire fault surfaces to the

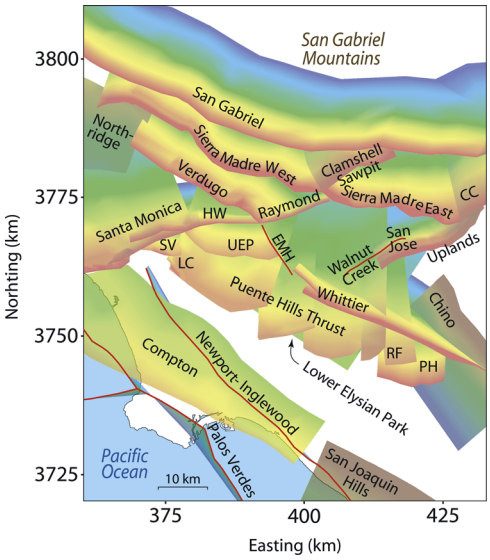

Figure 1. The three-dimensional active fault surfaces within the Los Angeles metropolitan region are color shaded to 27.5 km depth: warmer colors indicate shallower depths. Vertical faults are represented as red lines. Darker backlit surfaces are south-dipping. The tessellated fault surfaces are provided by the SCECs Community Fault Model (CFM) v. 2.5 [*Plesch et al.*, 2002]. CC = Cucamunga, HW = Hollywood, EMH = East Montebello Hills, RF = Richfield, PH = Peralta Hills, LC = Las Cienegas, SV = San Vicente and UEP = Upper Elysian Park.

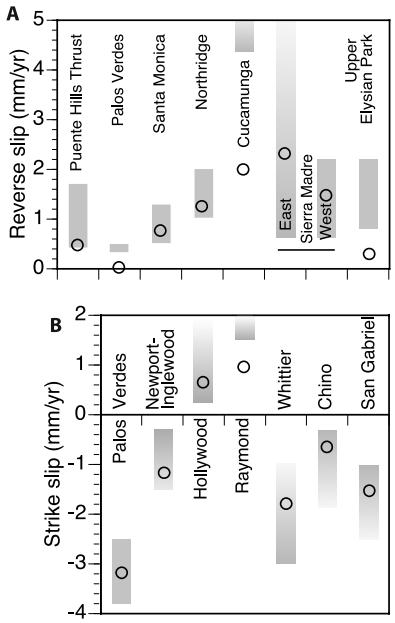

Figure 2. (a) Dip-slip rates and (b) reverse-slip rates along faults within the Los Angeles region for which geologic rates are known. Grey bars show ranges of geologic slip rates from paleoseismic studies for daylighting faults and inferences from deformation of overlying strata for blind faults (i.e., Puente Hills Thrust, Upper Elysian Park and Northridge faults). Ranges are lightly shaded where they are less confidently constrained. All but 3 of the 16 modeled average slip rates falls within the range of geologic values.

available geologic slip rates. Sense of strike-slip along faults in the geologic model matches the slip sense on all faults for which paleoseismic or geologic slip rate information is available (Figure 2). Furthermore, the strike-and dip-slip rates fall within the available ranges of geologic slip rates for 11 of the 15 faults (Figure 2). Previous models that only included faults within the seismogenic portion of the crust (<17 km depth) matched geologic slip sense on all faults but did not produce such close match the geologic slip rates [*Griffith and Cooke*, 2005]. The good correlation of geologic slip rates with results from models that include deformation below the seismogenic crust serves to validate the modeling approach of using a horizontal detachment to simulate lower crustal deformation.

[11] The BEM model is linear elastic and does not include the effects of compliant sedimentary fill within the Los Angeles basin, which could affect slip rates along nearby faults. While models of the Ventura basin better match geodetic data with compliant basin fill [*Hager et al.*, 1999], heterogeneous basin fill does not improve the fit to geodetic data within models of the Salton trough [*Fay and Humphreys*, 2005]. The close correlation of our three-dimensional model results with geologic slip rates suggests that the primary control on the distribution of geologic deformation within the Los Angeles basin is the configuration of the three-dimensional fault network. This suggestion is supported by the sensitivity of fault slip rates to changes in three-dimensional fault configuration even at depth greater than 8 km [*Griffith and Cooke*, 2004].

4. Insights From Slip Rate Discrepancies

[12] The modeled Upper Elysian Park fault reverse-slips 0.5 mm/yr slower than estimated from deformation of overlying Quaternary terrace deposits. [*Oskin et al.*, 2000]. This slip rate discrepancy is not likely due to slowing of fault slip rates between the time of terrace deposition and the present-day deformation simulated in the model; these terraces are dated at only 50–74 ka [*Oskin et al.*, 2000]. This discrepancy may, however, indicate inaccurate CFM v. 2.5 configuration of this and/or nearby faults. Alternative configurations of nearby faults have improved match of modeled surface uplift patterns to geologic uplift constrained from marker horizon depths within wells [*Cooke et al.*, 2004]. Such alternative fault configurations may also reduce mismatch of slip rates on the Upper Elysian Park and Raymond faults. Within the present model, the Raymond fault strike-slips 0.5 mm/yr slower than estimated from a three-dimensional trench survey [*Marin et al.*, 2000].

[13] The Cucamonga fault within the model has slip rates significantly lower than the geologic estimates [*Morton and Matti*, 1987]. This fault is located at the edge of the Los Angeles model and adjacent to the San Andreas fault, not included in our model. Incorporating the San Andreas and San Jacinto faults would interfere with the boundary conditions used in this study, which exclude from the geodetic signal the effect of the San Andreas and San Jacinto faults on the Los Angeles basin [*Argus et al.*, 2005]. While the boundary conditions simulate well slip rates on faults within the Los Angeles basin and distal to the San Andreas, discrepancies may arise on faults adjacent to the San Andreas, such as the Cucamonga fault.

[14] The average west-side-up-slip along the vertical modeled Palos Verdes fault is 0.3 mm/yr lower than that inferred from uplifted marine terraces along the Palos Verdes Peninsula [*Bryant*, 1987; *Ponti and Lajoie*, 1992]. The discrepancy reflects our comparison of the average dip-slip along the entire modeled Palos Verdes fault surface with geologic slip rates estimated within the local restraining

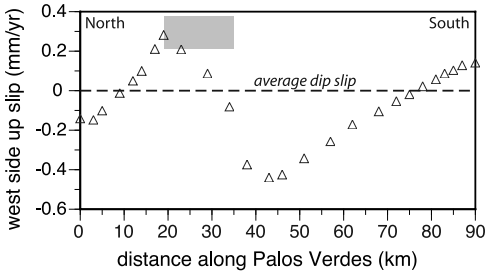

Figure 3. West-side-up-slip rate along the vertical Palos Verdes fault. The grey box shows the locations and range of slip rates determined from analysis of uplifted marine terraces along the Palos Verdes peninsula [*Bryant*, 1987; *Ponti and Lajoie*, 1992]. While the average modeled slip rate along the entire surface of the fault (dashed line) does not match the geologic slip rate, the modeled near surface west-side-up-slip rates near the areas of the geologic investigation fall within the range of geologic slip rates.

Table 3. Area-Weighted Average Slip Rates Along Modeled Fault Surfaces[a]

Fault	Dip, mm/yr	Strike, mm/yr	Net, mm/yr
Palos Verdes	**0.0**	**−3.2**	3.2
Sierra Madre (East)	**2.3**	−0.2	2.3
San Gabriel	1.7	**−1.5**	2.3
Cucamonga	**2.0**	0.8	2.1
Whittier/Glen Ivy	0.4	**−1.8**	1.8
Sierra Madre (West)	**1.5**	−0.6	1.6
Northridge	**1.2**	−0.4	1.3
Raymond	0.7	**1.0**	1.2
Newport-Inglewood	0.2	**−1.2**	1.2
Chino	1.0	**−0.6**	1.2
Hollywood	0.7	**0.7**	1.0
Santa Monica	**0.8**	0.6	1.0
Lower Elysian Park	0.6	−0.6	0.8
Verdugo-Eagle Rock	0.5	−0.6	0.8
Clamshell-Sawpit	0.3	0.7	0.8
San Jose - Uplands	0.3	0.6	0.7
Walnut Creek	0.2	0.6	0.6
East Montebello	0.3	−0.5	0.5
Peralta Hills	0.5	0.0	0.5
Puente Hills	**0.5**	0.0	0.5
Upper Elysian Park	**0.3**	−0.1	0.3
Redondo Canyon	0.0	−0.3	0.3
Compton	0.3	0.0	0.3
Richfield	0.2	0.1	0.2
San Vicente	0.2	0.0	0.2
Las Cienegas	0.0	−0.1	0.1

[a]Faults are sorted by net slip rates. Negative strike-slip rates are right-lateral and positive are left-lateral. Dip- and strike-slip rates in bold are compared to geologic rates (Figure 2); others are unconstrained by geologic evidence.

bend of this strike-slip fault. When we compare the geologic dip-slip rates with model predictions of near surface west-side-up-slip rates along the trend of the Palos Verdes fault, we see that along the restraining bend of the Palos Verdes peninsula, the model slip rates are more consistent with the geologic rates (Figure 3). Thus, the comparison of modeled slip rates at the site of the geologic investigation provides better match than the average slip rate along the entire fault surface. This implies that dip-slip rates estimated from marine terrace uplifts along the Palos Verdes peninsula may not represent the dip-slip along most of the Palos Verdes fault. Because the distribution of slip can be irregular along faults with non-planar topology, such as the restraining bend of the Palos Verdes fault, geologic slip rates determined at specific sites along non-planar faults may not necessarily reflect representative values [*Marshall et al.*, 2006].

[15] We expect that deepening the horizontal detachment within the model would slightly increase dip-slip rates along detachment-intersecting faults while strike-slip rates would remain unchanged; dip-slip may be restricted across intersections of steep faults with the horizontal detachment while strike-slip is more easily transferred to the detachment. Because changing the depth of the detachment would influence dip-slip rates on all faults, such changes would not greatly improve misfit to the geologic data, which match for most faults.

5. Slip Rates for Geologically Unconstrained Faults

[16] The match of the modeled fault slip rates with available paleoseismic and geologic data on 12 out of 15 faults validates the prediction of slip rates from these three-dimensional BEM models. Consequently, the model results provides 37 strike- and dip-slip rates along faults for which paleoseismic information is not available (Table 3). For example, the model predicts negligible overall strike-slip along the blind Puente Hills fault, confirming previous analyses of this as a primarily dip-slip structure [*Shaw et al.*, 2002]. Furthermore, in our model the Santa Monica, Sierra Madre and Cucamunga faults, which have well-documented reverse-slip, also display significant strike-slip, which has not yet been constrained and documented within geologic studies. Because strike-slip has not been recognized along these and other faults of the Los Angeles basin, the net-slip used for seismic hazard analysis may be underestimated. Some active faults in the Los Angeles basin have no geologic slip rates estimates at this time. For example, geologic slip rates are not available for the Verdugo/Eagle Rock fault though the net slip rate on this fault appears to be ~0.8 mm/yr (Table 3). Our model, which incorporates geologically realistic, three-dimensional representations of the regional faults, provides a comprehensive estimate of slip on faults within the Los Angeles basin and may provide the best available estimates of slip rates for unstudied faults. Such slip rates can be used in seismic hazard estimates of Southern California with the consideration that alternative fault configurations may provide different slip estimates.

6. Conclusions

[17] With very few exceptions, slip rates along all of the modeled three-dimensional faults match well the geologic rates available. The incorporation of geology-based non-planar representations of fault surfaces within the Los Angeles metropolitan region permits the model to capture the distribution of active three-dimensional deformation within the region. Alternative configurations of faults within the northern Los Angeles basin near the Upper Elysian Park and Raymond faults may provide better match to slip rates on these faults. Irregular slip distribution along the non-planar Palos Verdes fault yields slip rates at the specific sites of geologic investigation that match better the geologic rates than slip rates averaged along the entire fault surface. Consideration should be given to the estimation of representative slip rates along non-planar faults. This study provides validated dip-and strike-slip rate estimates for 26 active faults in the Los Angeles metropolitan region (Table 3). Many of these rates can be used to estimate seismic hazards on faults for which slip rates are unknown or underestimated.

[18] **Acknowledgments.** This paper was improved by reviews of Eric Hetland and an anonymous reviewer. This research was supported by the Southern California Earthquake Center (SCEC). SCEC is funded by National Science Foundation Cooperative Agreement EAR-0106924 and USGS Cooperative Agreement 02HQAG0008. This work is Southern California Earthquake Center report 1032. POLY3D was made available by IGEOSS. Manipulation of fault surfaces was facilitated by use of 3DMove by Midland Valley Ltd.

References

Argus, D., M. Heflin, G. Peltzer, F. Crampe, and F. Webb (2005), Interseismic strain accumulation and anthropogenic motion in metropolitan Los Angeles, *J. Geophys. Res.*, *110*, B04401, doi:10.1029/2003JB002934.

Bryant, M. E. (1987), Emergent marine terraces and Quaternary tectonics, Palos Verdes Peninsula, California, *SEPM Guidebook*, *55*, 63–78.

Cooke, M. L., A. Meigs, and S. T. Marshall (2004), Testing 3D fault configuration in the northern Los Angeles basin, California via patterns of rock uplift the since 2.9 Ma, *Eos Trans. AGU*, *84*(46), Abstract T11D-1296.

Fay, N., and E. D. Humphreys (2005), Fault slip rates, effects of elastic heterogeneity on geodetic data, and the strength of the lower crust in the Salton Trough region, southern California, *J. Geophys. Res.*, *110*, B09401, doi:10.1029/2004JB003548.

Fuis, G., T. Ryberg, N. J. Godfrey, D. A. Okaya, and J. M. Murphy (2001), Crustal structure and tectonics from the Los Angeles basin to the Mojave desert, southern California, *Geology*, *29*, 15–18.

Grant, L. B., and M. M. Gould (2004), Assimilation of Paleoseismic data for earthquake simulation, *Pure Appl. Geophys.*, *161*, 2295–2306.

Griffith, W. A., and M. L. Cooke (2004), Mechanical validation of the three-dimensional intersection geometry between the Puente Hills blind-thrust system and the Whittier fault, Los Angeles, California, *Bull. Seismol. Soc. Am.*, *94*, 493–505.

Griffith, W. A., and M. L. Cooke (2005), How sensitive are fault slip rates in the Los Angeles to tectonic boundary conditions?, *Bull. Seismol. Soc. Am.*, *95*, 1263–1275.

Hager, B. H., G. A. Lyzenga, A. Donnellan, and D. Dong (1999), Reconciling rapid strain accumulation with deep seismogenic fault planes in the Ventura Basin, California, *J. Geophys. Res.*, *104*, 25,207–25,219.

Maerten, F., P. Resor, D. Pollard, and L. Maerten (2005), Inverting for slip on three-dimensional fault surfaces using angular dislocations, *Bull. Seismol. Soc. Am.*, *95*, 1654–1665.

Magistrale, H., S. Day, R. W. Clayton, and R. Graves (2000), The SCEC Southern California reference three-dimensional seismic velocity model version 2, *Bull. Seismol. Soc. Am.*, *90*, S65–S76.

Marin, M., J. F. Dolan, R. D. Hartleb, S. A. Christofferson, A. Z. Tucker, and L. A. Owen (2000), A latest Pleistocene-Holocene slip rate on the Raymond Fault based on 3-D trenching, East Pasadena, California, *Eos Trans. AGU*, *81*(48), Fall Meet Suppl., Abstract S62B-03.

Marshall, S. T., M. L. Cooke, and S. E. Owen (2006), Three-dimensional fault topology in the Ventura Basin, California, and a new technique for creating three-dimensional interseismic mechanical models in complex regions, presented at the International Workshop on Comparative Studies of the North Anatolian Fault and the San Andreas Fault (Southern California), Istanbul Tek. Univ., Istanbul, Turkey.

Meade, B. J., and B. H. Hager (2005), Block models of crustal motion in Southern California constrained by GPS measurements, *J. Geophys. Res.*, *110*, B03403, doi:10.1029/2004JB003209.

Morton, D. M., and J. C. Matti (1987), The Cucamonga fault zone: Geologic setting and Quaternary history, in *Recent Reverse Faulting the Transverse Ranges, California*, edited by D. M. Morton and R. F. Yerkes, pp. 179–203, U.S. Geol. Surv., Boulder, Colo.

Muller, J. R., and A. Aydin (2005), Using mechanical modeling to constrain fault geometries proposed for the northern Marmara Sea, *J. Geophys. Res.*, *110*, B03407, doi:10.1029/2004JB003226.

Oskin, M., K. Sieh, T. Rockwell, G. Miller, P. Guptill, M. Curtis, S. McArdle, and P. Elliot (2000), Active parasitic folds on the Elysian Park anticline: Implications for seismic hazard in central Los Angeles, California, *GSA Bull.*, *112*, 693–707.

Plesch, A., et al. (2002), SCEC 3D Community Fault Model for Southern California, *Eos. Trans. AGU*, *83*(47), Fall Meet. Suppl., Abstract S21A-0966.

Ponti, D. J., and K. R. Lajoie (1992), Chronostratigraphic implications for tectonic deformation of Palos Verdes and Signal Hills, Los Angeles Basin, California, paper presented at 35th Annual Meeting, Assoc. of Eng. Geol., Long Beach, Calif.

Shaw, J., A. Plesch, J. Dolan, T. Pratt, and P. Fiore (2002), Puente Hills blind-thrust system, Los Angeles, California, *Bull. Seismol. Soc. Am.*, *92*, 2946–2960.

Thomas, A. L. (1994), POLY3D: A three-dimensional, polygonal element, displacement discontinuity boundary element computer program with applications to fractures, faults, and cavities in the Earth's crust, Master's thesis, 52 pp., Stanford Univ., Stanford, Calif.

Working Group on California Earthquake Probabilities (1995), Seismic hazards in southern California: Probable earthquakes, 1994 to 2024, *Bull. Seismol. Soc. Am.*, *85*, 379–439.

Wright, T. L. (1991), Structural geology and tectonic evolution of the Los Angeles Basin, California, in *Active Margin Basins*, *AAPG Mem.*, *52*, 35–134.

M. L. Cooke and S. T. Marshall, Geosciences Department, University of Massachusetts, Morrill Science Center, 611 North Pleasant Street, Amherst, MA 01003, USA. (cooke@geo.umass.edu)